RAMAN SCATTERING STUDY OF THE QUASI-ONE-DIMENSIONAL CONDUCTOR ZrTe_5 and HfTe_5(EXPERIMENTS ON MX_5 COMPOUNDS, International Symposium on NONLINEAR TRANSPORT AND RELATED PHENOMENA IN INORGANIC QUASI ONE DIMENSIONAL CONDUCTORS)

AUTHOR(S):

Taguchi, I.; Grisel, A.; Levy, F.

RAMAN SCATTERING STUDY OF THE QUASI-ONE-DIMENSIONAL CONDUCTOR $ZrTe_5$ and $HfTe_5$

I. Taguchi*, A. Grisel and F. Lévy
Institut de Physique Appliquée, EPF, Lausanne, Switzerland

By Raman scattering, seven vibrational modes have been detected for $ZrTe_5$, whereas nine for $HfTe_5$. The application of a central force model reveals the characteristic vibrational-modes in the transition-metal pentatellurides. The comparison of the observed and calculated frequencies shows the reduction of the strength of the pairing interaction between the chalcogen atoms within the prismatic chain compared to $ZrTe_3$ and the weakness of the interaction in the tellurium zig-zag chain. The temperature dependence of the half widths shows an unusual increase of the spectral density at low temperatures. The obtained results suggest the existence of two structural distortions or transitions: one occurs above room temperature and the other is related with the reported resistivity anomaly at low temperatures.

I. INTRODUCTION

Recently, the transition-metal pentatellurides $ZrTe_5$ and $HfTe_5$ have received much attention as new quasi-one-dimensional conductors which show anomalous transport properties. Similarly with the transition-metal trichalcogenides, these crystals have the trigonal prism as the basic structural element, which is parallel to the c-axis and is composed of the tellurium atoms at its corners and of the metal atom at its center. The difference originates from the way of coupling between the neighbouring prismatic chains: in the trichalcogenides, the chains are directly linked by metal-chalcogen bonds to create layers, whereas, in the pentatellurides, they interact with each other through the zig-zag chain along the c-axis which is composed of tellurium atoms [1].

The remarkable property of the lattice dynamics of the transition-metal trichalcogenides is the combination of the one- and two-dimensional feature of

* Present address: Department of Physics, Shimane Medical University, Izumo 693, Japan

the lattice vibrations [2,3]. In the present paper, we investigate the long-wavelength lattice vibrations of the pentatellurides using Raman scattering and a central force model for the lattice dynamics.

The presence of the Te-Te zig-zag chain is responsible for the metallic behaviour of the pentatellurides. Both $ZrTe_5$ and $HfTe_5$ exhibit a large resistivity anomaly [4,5] and change of the sign in the Hall coefficient [6] around 141 K (for $ZrTe_5$) and 83 K (for $HfTe_5$). These results are to be compared with those of a typical linear-chain metal $NbSe_3$ [7] which has a similar crystal structure and undergoes charge-density-wave transitions at low temperatures. Recent X-ray diffraction and magnetic measurements reported no evidence for a charge- or spin-density-wave transition for $ZrTe_5$ [8,9]. In contrast, it was found in other X-ray study [10] of $ZrTe_5$ and $HfTe_5$ that the intensities of some forbidden reflections show a large maximum correlated with the occurrence of the resistivity peak. We also examine the Raman spectra at low temperatures to obtain information about the possibility of phase transition or structural change in the pentatellurides.

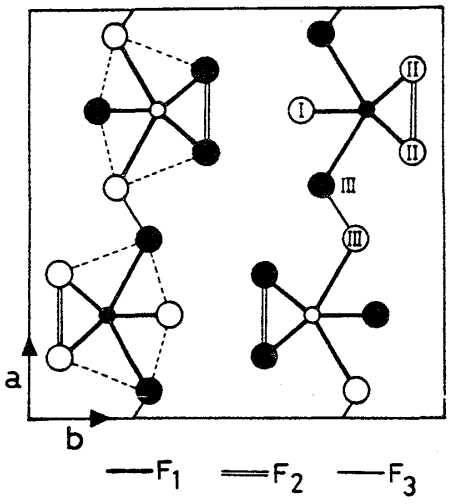

Fig.1. Crystal structure of the pentatellurides projected onto the (001) plane. The small and large circles denote the metal and tellurium atoms respectively. The two neighbouring ab planes which accommodate the open and solid circles, respectively, are separated by c/2. The proposed central force model assumes three kinds of interactions which are represented by —, ═ and —. The dotted line indicates the extended chain corresponding with the coordination number 8 for the metal atom.

According to the results of the structural determination by Furuseth et al.[11], $ZrTe_5$ and $HfTe_5$ are isostructural with each other and crystallize in an orthorhombic structure with the space group $C_{mcm}(D_{2h}^{17})$. The unit cell dimensions are a=13.727 Å, b=14.502 Å, c=3.9876 Å for $ZrTe_5$, and a=13.730 Å, b=14.492 Å, c=3.9743 Å for $HfTe_5$. Figure 1 shows the projection of the crystal structure of the pentatellurides onto the (001) plane. Since the distance between the metal and Te(III) atoms, 2.960 Å for $ZrTe_5$, is nearly equal to that between the metal and Te(I) atoms, 2.959 Å, or that between the metal and Te(II) atoms, 2.948 Å, within the prismatic chain, the metal atom is considered to be coordinated with eight chalcogen atoms rather than six. Therefore, we

regard the prismatic chain which is extended to include the Te(III) atoms at its both sides as the single chain which should be correlated with the crystal in the group analysis. In the actual crystals, these extended chains are connected to form layers, which are weakly coupled by forces of the van der Waals type.

Table 1. Correlation diagram for the transition-metal pentatellurides

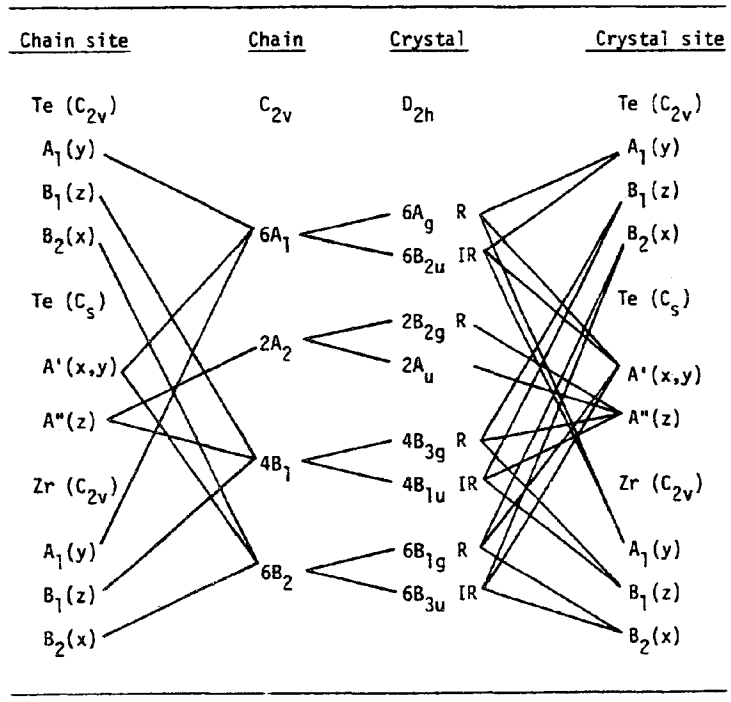

The symmetries of the long-wavelength phonons of the chain and crystal are given by [12,13]

$$\Gamma_{chain} = 6A_1 + 2A_2 + 4B_1 + 6B_2, \qquad (1)$$

$$\begin{matrix} & y & & z & R_z;x \\ x^2,y^2,z^2 & xz & & yz & xy \end{matrix}$$

$$\Gamma_{crystal} = 6A_g + 6B_{2u} + 2B_{2g} + 2A_u + 4B_{3g} + 4B_{1u} + 6B_{1g} + 6B_{3u}, \qquad (2)$$

$$\begin{matrix} & y & & & z & R_z & x \\ x^2,y^2,z^2 & & xz & & yz & xy & \end{matrix}$$

where transformation properties are described underneath each representation. Table 1 shows the correlation diagram for the pentatellurides [12]. Because of the presence of the inversion center, Raman and infrared activities are mutually exclusive. The $2B_{2g} + 4B_{3g}$ Raman and $4B_{1u}$ infrared modes have their atomic displacements along the c-axis, and the $6A_g + 6B_{1g}$ Raman and $6B_{2u} + 6B_{3u}$ infrared modes have their displacements perpendicular to the c-axis.

II. RAMAN SPECTRA AT ROOM TEMPERATURE

Single crystals of $ZrTe_5$ and $HfTe_5$ were grown by chemical transport reactions with iodine as a transport agent [14]. Raman spectra were obtained from freshly cleaved surfaces of the samples with the excitation from 5145 Å line of an argon-ion laser. Scattering experiments were performed in the forward scattering geometry, where the incident beam made about 30° against the sample surface to be examined. The scattered light collected at 90° with regard to the incident beam was analyzed by a Spex double spectrometer equipped with holographic gratings and polarization scrambler, and was detected by a photon counter. An Oxford continuous-flow cryostat was used for low temperature measurements.

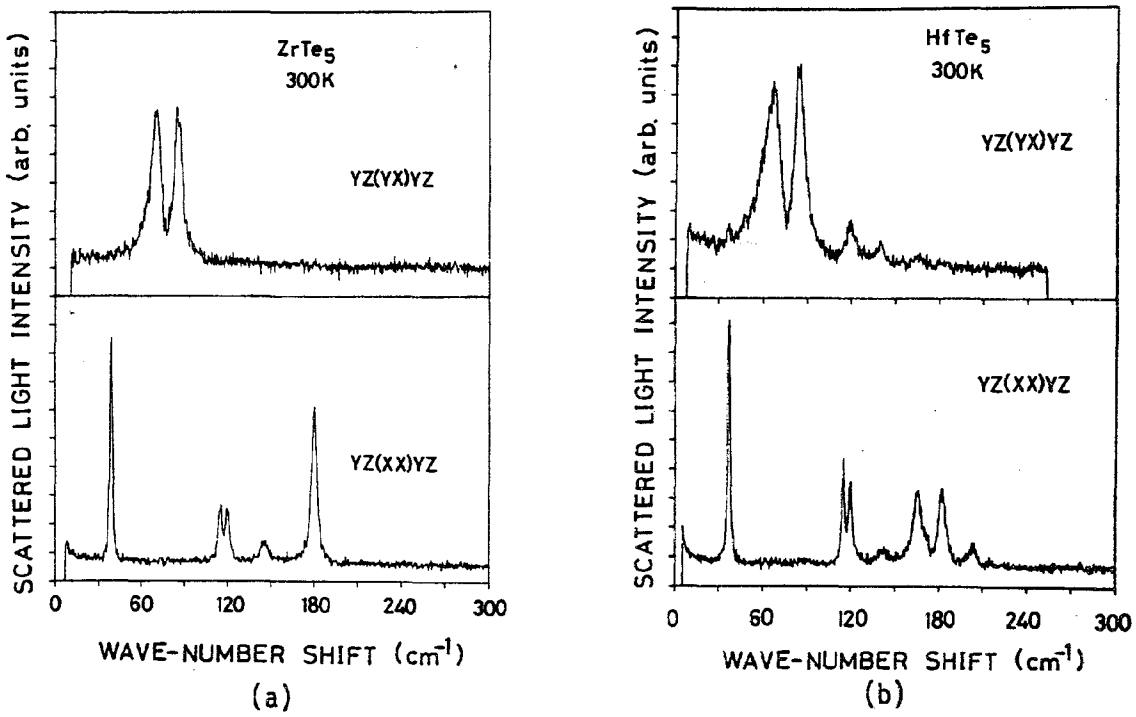

Fig.2. Polarized Raman spectra of (a) $ZrTe_5$ and (b) $HfTe_5$ at room temperature with the excitation from the 5145 Å line of an argon-ion laser.

Table 2. Raman frequencies of $ZrTe_5$ and $HfTe_5$ compared with the central force dynamical model

Vibrational symmetry		$ZrTe_5(cm^{-1})$			$HfTe_5(cm^{-1})$	
Chain	Crystal	Calc.	Meas.	Ref.15	Calc.	Meas.
			(235)			204
						182
A_1(diatomic)	A_g	179	179	181.5	166	166
B_1	B_{3g}	157	-	-	150	-
B_2	B_{1g}	151	-	-	145	-
A_1	A_g	149	143	144	138	140
A_1	A_g	97	119	121	96	119
B_2	B_{1g}	93	-	-	92	-
A_2/B_1(shearing;zig-zag chain)	B_{2g}/B_{3g}	84	84	87*	84	84
A_2/B_1(shearing)	B_{2g}/B_{3g}	69	69	72*	66	66
A_1	A_g	67	115	116	65	115
B_2	B_{1g}	67	-	-	65	-
A_1	A_g	58	-	-	56	-
B_2	B_{1g}	0	-	-	0	-
B_2	B_{1g}	0	-	-	0	-
A_1(rigid-chain/acous.)	A_g	0	39	39	0	37
B_1(rigid-chain/acous.)	B_{3g}	0	-	-	0	-
B_2(rigid-chain/acous.)	B_{1g}	0	-	-	0	-

* In ref.15, these two frequencies were regarded as crystal doublets resulted from the A_2 mode of the chain.

Figure 2 shows the polarized Raman spectra of $ZrTe_5$ and $HfTe_5$ at room temperature. One of the conspicuous results is the disagreement of the number of observed lines between $ZrTe_5$ and $HfTe_5$. In the configuration YZ(XX)YZ, five structures are detected for $ZrTe_5$, while seven for $HfTe_5$. Two structures are observed in the YZ(YX)YZ or XY(YZ)XY configuration for both materials. A comparison of the polarized spectra at low temperatures confirms the 179 cm^{-1} line in $ZrTe_5$ to correspond to the 166 cm^{-1} line in $HfTe_5$ [13].

The high frequency part of the spectra is also puzzling. In the case of the transition-metal trichalcogenides, the spectra include the characteristic diatomic mode which is very intense and has the highest frequency. This mode is related with the stretching motion of the chalcogen atoms paired on the shortest side of the prismatic chain. Since the distance between the Te(II)-

Te(II) atoms is nearly equal among $ZrTe_3$, $ZrTe_5$ and $HfTe_5$ (2.761 Å, 2.762 Å, 2.763 Å, respectively), we could expect a strong line around 216 cm^{-1} which is the corresponding frequency for $ZrTe_3$ [3]. However, the highest frequency line actually observed has much lower frequency: 204 cm^{-1} for $HfTe_5$ and 179 cm^{-1} for $ZrTe_5$. Table 2 lists the frequencies of all the peaks together with the data on $ZrTe_5$ by Zwick et al. [15].

III. A CENTRAL FORCE MODEL

In order to interpret the experimental data, we use a central force model for the lattice vibrations. We first consider the case of $ZrTe_5$. The model assumes three kinds of interactions which are explained in Fig.1. The metal atom interacts with the eight tellurium atoms. On the basis of the structural analysis by Furuseth et al. [11], the atomic distance is nearly equal among metal-Te(I), metal-Te(II) and metal-Te(III). Therefore, we assume these eight interactions to be described by the single force constant F_1. Pairing between the Te(II) atoms within the prismatic chain is characterized by the force constant F_2. The third force constant, F_3, characterizes the interaction between the Te(III) atoms in the zig-zag chain or, in other words, the interaction between the extended prismatic chains.

The thirteen k=0 normal vibrations of the crystal are schematically drawn in Fig.3. The magnitude of the displacement vectors applies to $ZrTe_5$. Positive and negative sign in the B_1 and A_2 modes indicate the atomic displacements parallel and antiparallel, respectively, to the axis of the prisms. With respect to reflection across the plane which is perpendicular to the page and includes the metal and Te(I) atoms, the $5A_1 + 3B_1$ modes are symmetric and the the $2A_2 + 3B_2$ modes are antisymmetric. The two B_2 modes and $A_1 + B_1 + B_2$ quasi-rigid acoustical modes have zero frequency. The central force model for the pentatellurides does not have restoring forces enough to describe such low frequency modes.

It is worth while noting that the central force model shows the degeneracy of the two shearing modes, A_2 and B_1, which are associated with the parallel or antiparallel motion of the tellurium atoms within the chain (number 7 and 10, respectively, in Fig.3). These degenerate vibrations demonstrate the one-dimensional feature of the crystals of the pentatellurides. In fact, this type of degeneracy is normally observed in the trichalcogenides [2,3] and, in the case of $ZrTe_3$, at 64 cm^{-1} [3]. Thus, we can correctly assign the 69 cm^{-1} line observed in $ZrTe_5$ to the A_2 degenerate mode. This identification determines the strength of the force constant F_1. Moreover, in the case of the

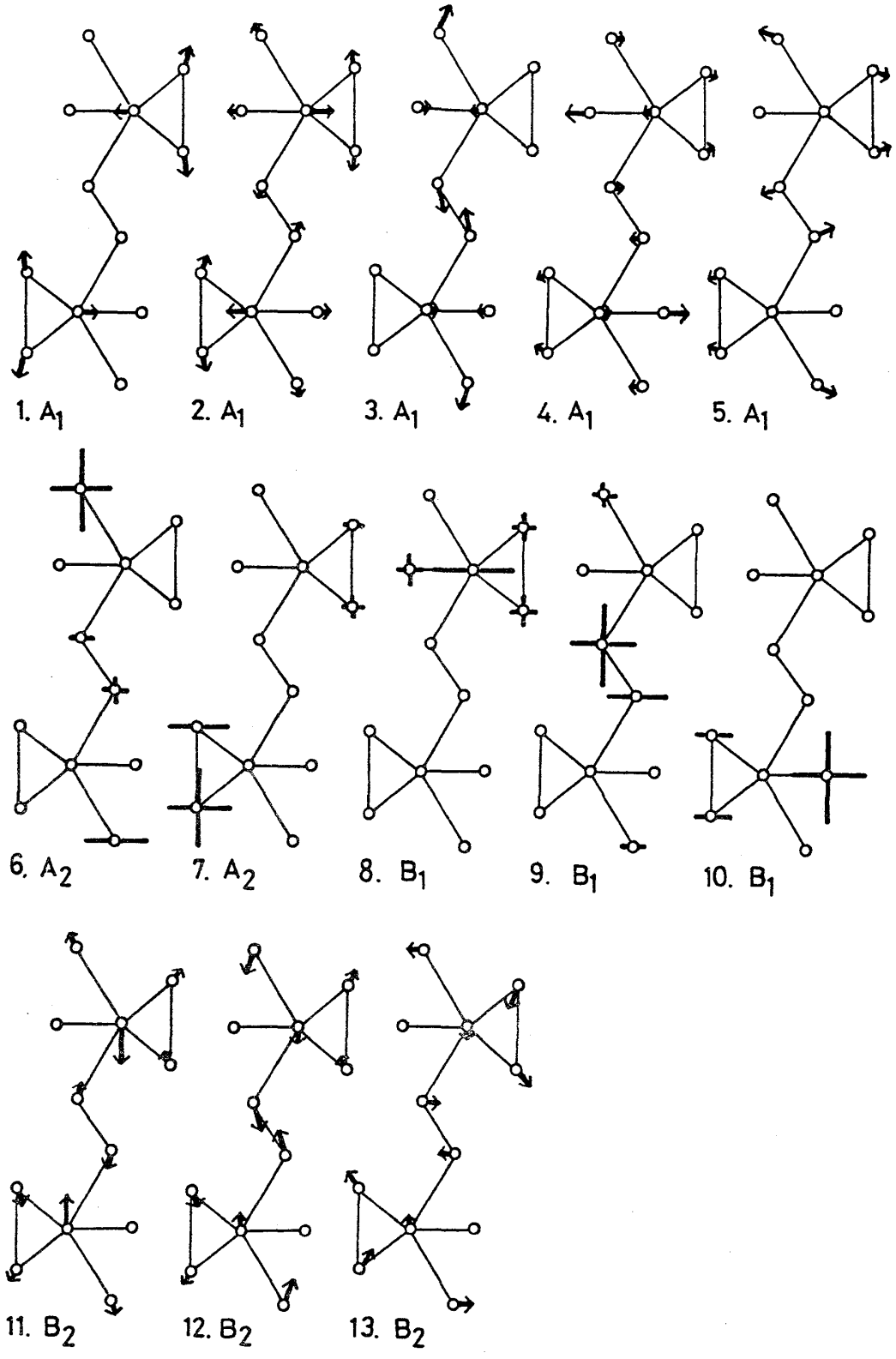

Fig.3. Thirteen k=0 normal vibrations of $ZrTe_5$. Positive and negative sign indicate the atomic displacements parallel and antiparallel, respectively, to the c-axis.

pentatellurides, we notice the existence of another degeneracy of the one-dimensional modes A_2 and B_1 (number 6 and 9, respectively, in Fig.3) which indicates the shearing motion of the Te(III)-Te(III) zig-zag chain along the c-axis. The polarized spectra show that the 84 cm^{-1} peak detected in the YZ(YX)YZ configuration is related to these degenerate modes. The fitting of this frequency gives the strength of the force constant F_3.

In the trichalcogenides, the highest-frequency line is associated with the chalcogen-chalcogen diatomic mode [2,3]. The present force model for the pentatellurides offers a similar diatomic mode (number 1 in Fig.3). We assign the intense line with the highest frequency of 179 cm^{-1} to this mode, from which the value of F_2 is calculated. Using these values of the force constants, we can calculate all the frequencies and the corresponding atomic displacements of the lattice modes, which allows us to assign the rest of the Raman peaks. The comparison of the result of the calculation with the Raman data is shown in Table 2. The agreement between the calculated and observed frequencies is reasonably good except for the 115 cm^{-1} line and for the low-frequency modes.

As regards the assignment of the 115 cm^{-1} peak, the discrepancy seems to be too large even if we consider the simpleness of the force model. In this connection, the fact that the 115 cm^{-1} peak locates close to the 119 cm^{-1} peak can force us to regard the 115 cm^{-1} peak as the B_2 mode (number 12 in Fig.3). This assignment, however, implies the breakdown of the prediction by the selection rule, which means that the symmetry of the lattice sensed instantaneously by the Raman scattering is different from C_{mcm}. It is also possible that the inversion center is lost in the instantaneous crystal symmetry. Since, in this case, both gerade and ungerade modes under the centrosymmetric structure become Raman active, the peak at 115 cm^{-1} could be attributed to the A_1 ungerade mode. Although which would be the actual case is uncertain at present, it is possible that this problem is correlated with the existence of some structural change even at room temperature.

The Raman frequencies of $HfTe_5$ have correspondences with those of $ZrTe_5$ except for the two highest-frequency ones. The reason of the appearance of the extra lines is not clear. It seems to originate also from such a change in the crystal symmetry as mentioned above or from polytypism. The result of the comparison of the observed and calculated frequencies for $HfTe_5$ is shown in Table 2.

Table 3 lists the determined strengths of the force constants. The comparison with the results of the trichalcogenides gives the following information about the chemical bonds: (1) the strengths of the eight bonds

Table 3. Strengths of the force constants used in the central force model for $ZrTe_5$ and $HfTe_5$ compared with those of $ZrTe_3$

Crystal	Force constants (dyn/cm)		
	F_1	F_2	F_3
$ZrTe_5$	3.9×10^4	9.8×10^4	2.9×10^4
$HfTe_5$	3.6×10^4	7.7×10^4	2.9×10^4
$ZrTe_3$	3.4×10^4	1.6×10^5	(3.1×10^4)

within the prismatic chain in $ZrTe_5$ or $HfTe_5$ are practically the same as those in $ZrTe_3$. (2) The Te(II)-Te(II) paring interaction is substantially weaker in the pentatellurides than in the trichalcogenides. (3) The strength of the interaction contributing to the Te(III) zig-zag chain is relatively weak. The last result is consistent with the fact that the Te(III)-Te(III) distance roughly corresponds to a half bond [1].

IV. TEMPERATURE DEPENDENCE OF THE RAMAN SPECTRA

Figure 4 shows the temperature dependence of the Raman spectra of $HfTe_5$. The spectra of $ZrTe_5$ exhibit a similar temperature dependence [13,15]. While the frequency of each line varies continuously with temperature, the half width shows an intriguing temperature dependence as is shown in Fig.5. When temperature is lowered, the half widths of some lines linearly decrease, but remain approximately constant below the temperature, T_p, at which the resistivity takes the maximum. The unusual increase of the spectral density means the breakdown of the k=0 selection rule and, therefore, suggests the occurrence of some structural change below T_p. Furthermore, it may show the possibility of charge-density-wave transitions because, similarly to the present case of the pentatellurides, no new line is detected in the low temperature Raman spectra of $NbSe_3$ which really undergoes charge-density-wave transitions [16]. The lines which show the large temperature dependence of the half width are the 140, 84 and 66 cm^{-1} lines that are connected to the lattice modes with the displacements of both Te(II) and Te(III) atoms. Thus it is suggested that both the Te(III) zig-zag chain and prismatic chain are affected by the possible distortion. In contrast, the 37 cm^{-1} line shows no significant temperature dependence, which implies that it is related to one of the external modes as is assigned in Table 2.

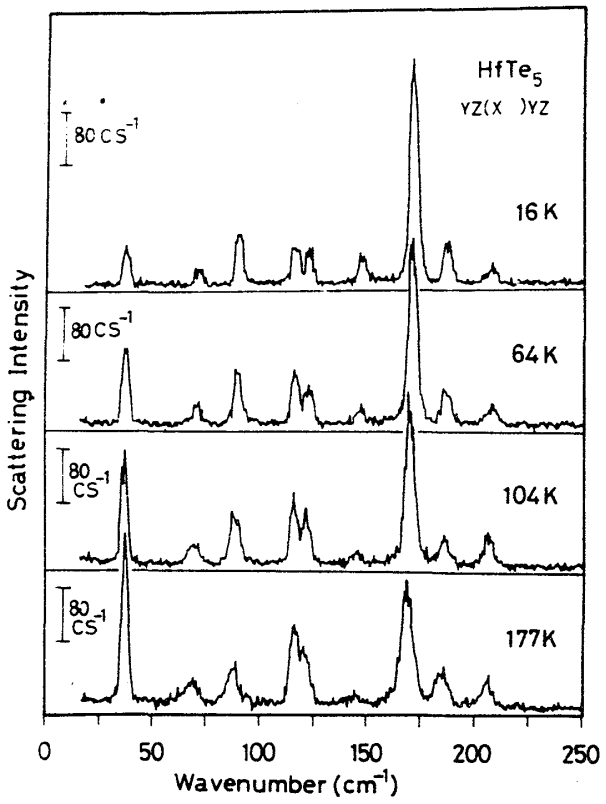

Fig.4. Temperature dependence of the unpolarized spectra of $HfTe_5$ excited with the 5145 A line from an argon-ion laser.

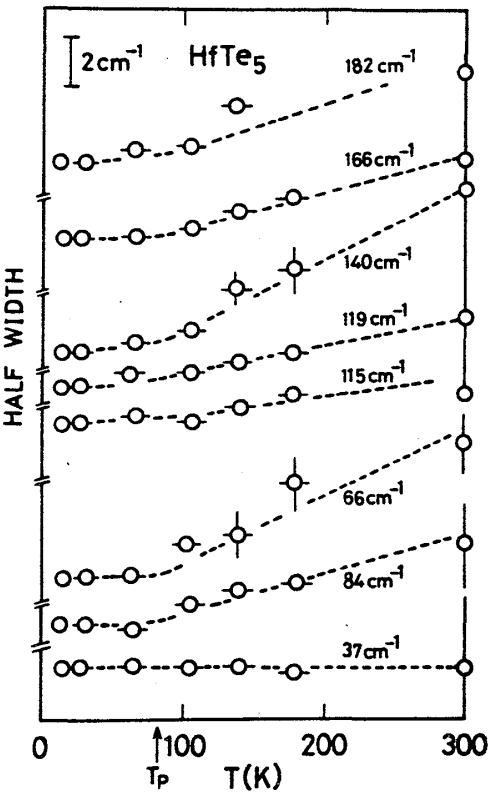

Fig.5. Temperature dependence of the half widths of the Raman lines for $HfTe_5$.

V. CONCLUSION

The investigation of the long-wavelength phonons in $ZrTe_5$ and $HfTe_5$ by means of Raman scattering and a central force model has elucidated the lattice properties of the transition-metal pentatellurides. The temperature dependence of the half widths of the Raman lines and the large discrepancy between the calculated and observed frequency for the 115 cm^{-1} line suggest the occurrence of two structural transitions or distortions: one appears above room temperature and the other is responsible for the resistive anomaly at low temperatures. In connection with the former transition, it is to be noted that extra Bragg spots exist in the room-temperature X-ray diffraction patterns of $ZrTe_5$ and $HfTe_5$ [8,9,10].

Acknowledgements - One of the authors (I. Taguchi) wishes to thank Professor E. Mooser and Dr. W. Czaja for useful discussion and their continuous supports. They are grateful to Mr. H. Berger for growing single crystals and to Dr. T.J. Wieting for helpful discussions.

REFERENCES

1. F. Hulliger, Structural Chemistry of Layered-Type Phases (edited by F. Lévy), p.250, Reidel, Dordrecht (1976).
2. A. Grisel, F. Lévy and T.J. Wieting, Physica 99B, 365 (1980).
3. T.J. Wieting, A. Grisel and F. Lévy, Physica 105B, 366 (1981).
4. S. Okada, T. Sambongi and M. Ido, J. Phys. Soc. Japan 49, 839 (1980).
5. T.J. Wieting, D.U. Gubser, S.A. Wolf and F. Lévy, Bull. Am. Phys. Soc. 25, 340 (1980).
6. M. Izumi, K. Uchinokura, E. Matsuura and S. Harada, Solid State Commun. 42, 35 (1982).
7. N.P. Ong and P. Monceau, Phys. Rev. B16, 3443 (1977).
8. F.J. DiSalvo, R.M. Fleming and J.V. Waszczak, Phys. Rev. B24, 2935 (1981).
9. S. Okada, T. Sanbongi, M. Ido, Y. Tazuke, R. Aoki and O. Fujita, J. Phys. Soc. Japan 51, 460 (1982).
10. E.F. Skelton, T.J. Wieting, S.A. Wolf, W.W. Fuller, D.U. Gubser, T.L. Francavilla and F. Lévy, Solid State Commun. 42, 1 (1982).
11. S. Furuseth, L. Brattas and A. Kjekshus, Acta. Chem. Scand. 27, 2367 (1973).
12. I. Taguchi, A. Grisel and F. Lévy, Solid State Commun. 45, 541 (1983).
13. I. Taguchi, A. Grisel and F. Lévy, Solid State Commun. 46, 299 (1983).
14. F. Lévy and H. Berger, J. Cryst. Growth 61, 61 (1983).
15. A. Zwick, G. Landa, R.Carles, M.A. Renucci and A. Kjekushus, Solid State Commun. 44, 89 (1982).
16. S. Sugai, T. Taguchi and J. Nakahara, private communication (1983).